Source mechanisms of the 2004 Baladeh (Iran) earthquake sequence from Iranian broadband and short-period data and seismotectonic implications

S. Donner [1], D. Rößler [2], F. Krüger [1], A. Ghods [3], M. Strecker [1]

[1] University Potsdam, [2] Technical University of Denmark, [3] Inst. for Advanced Studies in Basic Sciences, Iran

contact: stefanie.donner@uni-potsdam.de

Introduction

The northward movement and collision of the Arabian plate with the Eurasian plate generates **compressive stresses** in Iran. Within the Alborz Mountains, North Iran, a **complex and not well understood system of strike-slip and thrust faults** accomodates a fundamental part of the NNE-SSW oriented shortening. On **28 May 2004, the Mw 6.3 Baladeh earthquake** hit the north-central Alborz Mountains. It is **one of the rare large events** in this region in modern times and thus a **unique chance to study earthquake mechanisms and the current local ongoing deformation processes.** This poster presents inversion results of the mainshock and 16 aftershocks.

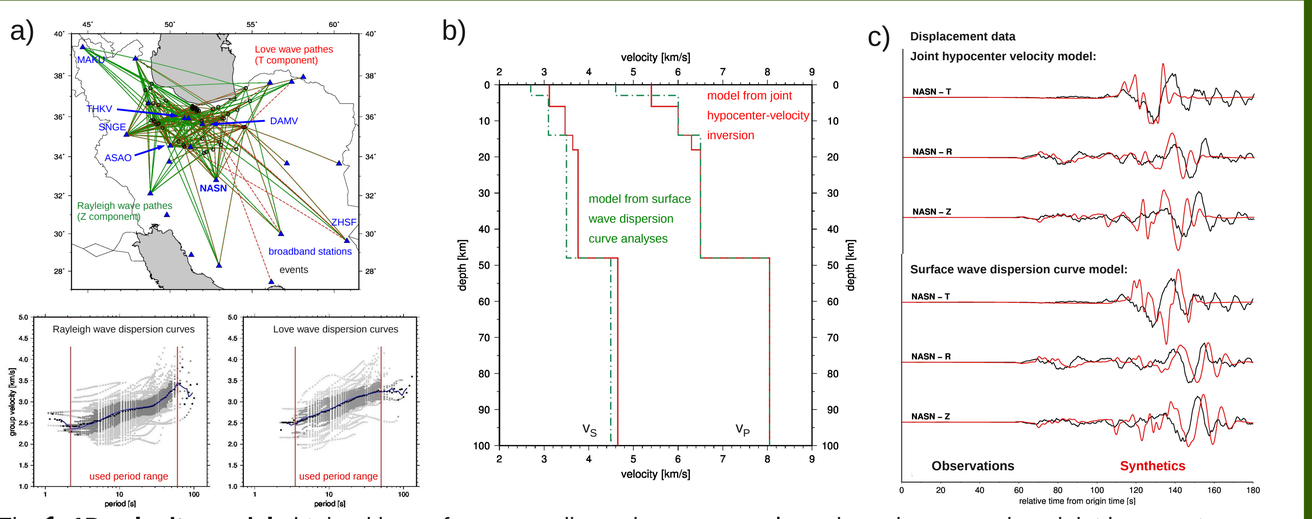

Fig. **1**: **1D velocity model** obtained by surface wave dispersion curve analyses based on a previous joint hypocenter-velocity inversion study: a) surface wave ray paths and group velocity dispersion curves (light grey - all dispersion curves; dark grey - curves within 1σ standard deviation; black/blue - median dispersion curve); b) velocity models in comparison; c) waveform comparison for both models with calculated synthetics.

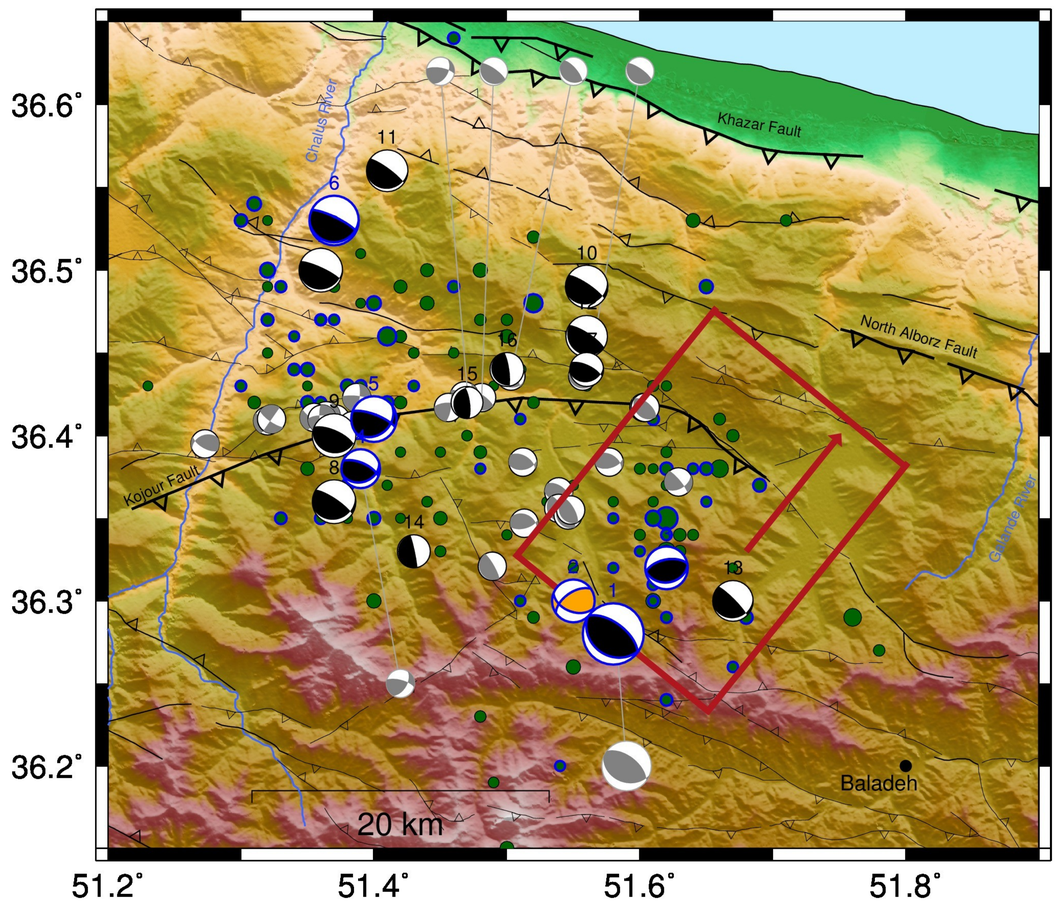

Fig. **4**: **Area map with solutions**. Event 1 is the mainshock. Red rectangle marks the horizontal projection of the rupture plane dipping 30°. All aftershocks with MN ≥ 2 (Nuttli magnitude) located by Iranian Seismological Centre (IRSC) are marked by green dots. Aftershocks (dots and solutions) marked in blue occured within 24h after the mainshock. Aftershocks marked in orange are located on the rupture plane. Grey focal solutions from Tatar et al. (2007).

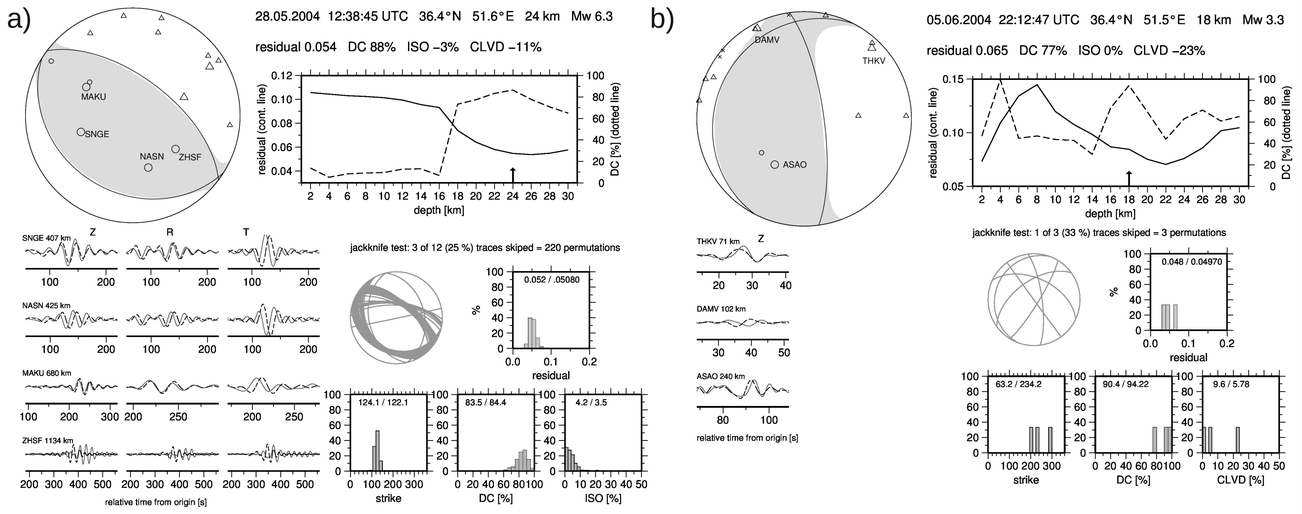

Fig. **2**: Examples of **point source frequency domain inversion results** for the mainshock (a) and three different aftershocks (b-d). Inversion was done between 0.01 and 0.1 Hz. For inversion of the aftershocks, isotropic constraint was used. Focal plane solutions show the solutions compared to P-wave polarities of broadband and short-period stations, a depth test, the forward calculated waveforms, and the results of a jackknife test. Compare figure to figure 4.

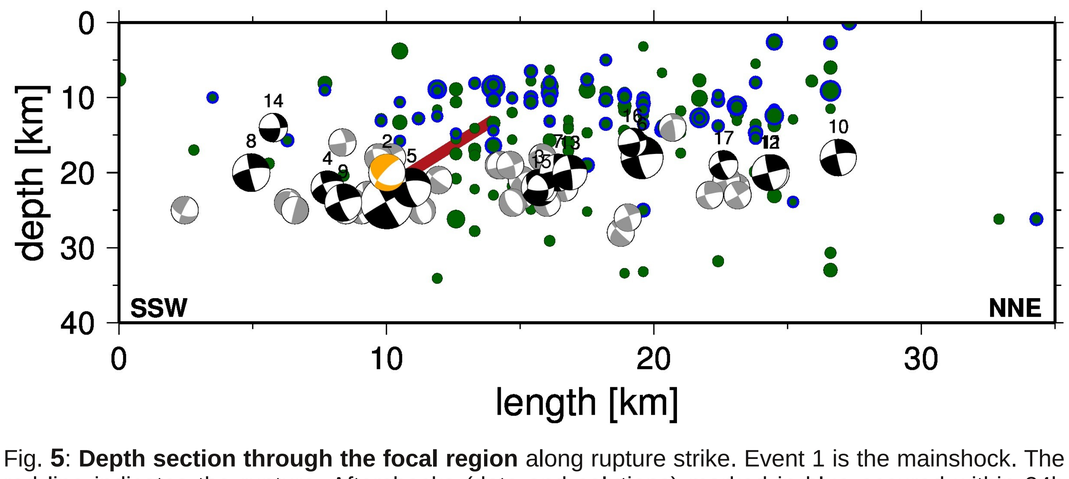

Fig. **5**: **Depth section through the focal region** along rupture strike. Event 1 is the mainshock. The red line indicates the rupture. Aftershocks (dots and solutions) marked in blue occured within 24h after the mainshock. Aftershocks marked in orange are located on the rupture plane.

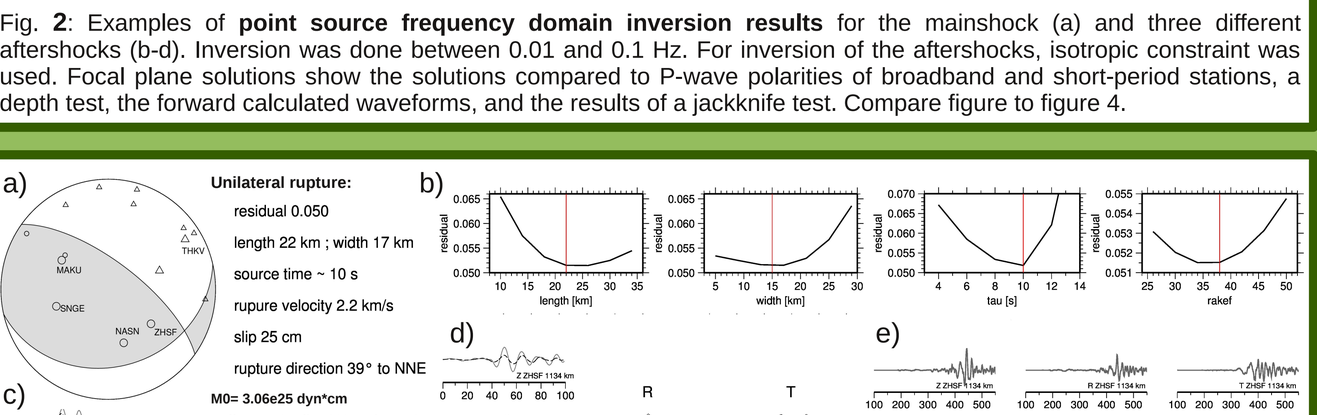

Fig. **3**: **Kinematic parameters of the mainshock** obtained by frequency spectra inversion for higher-degree moment tensor (Dahm & Krüger; 1999): a) solution; b) sensitivity tests; c) forward calculated surface wave waveforms; d) forward calculated body wave waveforms; e) pure restituted and unfiltered displacement data. For c) – e) time is in seconds.

Preliminary interpretation

The mainshock and the 16 analysed aftershocks show **almost pure reverse mechanisms** with an **average strike of NW-SE**. Dipping at ~ 30° the **rupture propagates from 24 km depth upward in NNE direction** with a length and width of 22 and 17 km and a rupture velocity of 2.2 km/s. The **slip was calculated to 25 cm**.

Using a double-couple constraint for the **point source inversion of** the **mainshock** results in a residual of 0.111 **compared to** a residual of 0.050 of the **extended source** double-couple **inversion**. Compared to the point source, the **extended source result shows a small left-lateral strike-slip component** in the solution.

Only 1 of the analysed aftershocks is located on the rupture plane. The remaining 15 **aftershocks are located within the footwall of the rupture**. In the West, the aftershock sequence stops at a distinct **river valley**, what seems to be a **segment boundary**. The largest aftershock (event 6 in fig. 4) with Mw 5.1 is also located here. The **orientation of the rupture plane** and the rupture direction seem to **contradict the aftershock distribution**.

Despite the concrete kinematic parameters of the rupture it is still **not possible to determine which fault has accommodated the rupture** since the fault system is highly complex. The candidates are the Khazar fault or the North Alborz fault close to the South Caspian Basin.

The **hypocentral depths** of the events between 14 and 24 km are remarkably deep. However, we interpret the events to be still located **in the upper crust**, right **above the midcrustal boundary**. The lower crust seems to be aseismic. This is supported by the overal seismicity distribution, which is shallower than 30 km.

Acknowledgement:

We are grateful to IASBS Zanjan for cooperation. We thank Prof. W. Friederich, Ruhr University Bochum, for kind assistance in interpretation of the surface wave dispersion curve.

We acknowledge Dr. R. Engdahl, University of Colorado; ETH Zürich; IIEES Tehran; Iranian Seismological Center; ISMN Tehran; ISC; EMSC, NOAA, and Harvard for providing earthquake catalogues and waveform data.

Reference:

Dahm, T.; Krüger, F. (1999) Higher-degree moment tensor inversion using far-field broad-band recordings: theory and evaluation of the method with application to the 1994 Bolivia deep earthquake. GJI Vol. 137 p. 35-50

Tatar, M.; Jackson, J.; Hatzfeld, D.; Bergmann, E. (2007) The 2004 May 28 Baladeh earthquake (Mw 6.2) in the Alborz, Iran: overthrusting the South Caspian Basin margin, partitioning of oblique convergence and the seismic hazard of Tehran. GJI Vol. 170 p. 249-261